Eur. Phys. J. Special Topics **224**, 2787–2801 (2015)

DOI: 10.1140/epjst/e2015-02589-1

THE EUROPEAN PHYSICAL JOURNAL SPECIAL TOPICS

Regular Article

Chaos control applied to piezoelectric vibration-based energy harvesting systems

W.O.V. Barbosa[1,a], A.S. De Paula[1,a], M.A. Savi[2,b], and D.J. Inman[3,c]

[1] Department of Mechanical Engineering, Universidade de Brasília, 70.910.900 Brasília, DF, Brazil
[2] Center for Nonlinear Mechanics, COPPE – Department of Mechanical Engineering, Universidade Federal do Rio de Janeiro, PO Box 68.503, 21.941.972 Rio de Janeiro, RJ, Brazil
[3] Department of Aerospace Engineering, University of Michigan, Ann Arbor, MI, USA

Received 15 July 2015 / Received in final form 9 September 2015
Published online 20 November 2015

Abstract. Chaotic behavior presents intrinsic richness due to the existence of an infinity number of unstable periodic orbits (UPOs). The possibility of stabilizing these periodic patterns with a small amount of energy makes this kind of response interesting to various dynamical systems. Energy harvesting has as a goal the use of available mechanical energy by promoting a conversion into electrical energy. The combination of these two approaches may establish autonomous systems where available environmental mechanical energy can be employed for control purposes. Two different goals can be defined as priority, allowing a change between them: vibration reduction and energy harvesting enhancement. This work deals with the use of harvested energy to perform chaos control. Both control actuation and energy harvesting are induced employing piezoelectric materials, in a simultaneous way. A bistable piezomagnetoelastic structure subjected to harmonic excitations is investigated as a case study. Numerical simulations show situations where it is possible to perform chaos control using only the energy generated by the harvesting system.

1 Introduction

Piezoelectricity is related to smart materials that present an electromechanical coupling, making it possible the conversion of mechanical into electrical energy and vice-versa (see for example: Leo, 2007). The direct effect is related to a mechanical strain that leads to a distribution of electrical charges on the surface of the material. This effect is usually explored to produce sensors. Another important application of this kind of behavior is the energy harvesting where available mechanical energy is converted into electrical energy (Erturk & Inman, 2008a; Tang et al., 2010;

[a] e-mail: alinedepaula@unb.br
[b] e-mail: savi@ufrj.br
[c] e-mail: daninman@umich.edu

Gkoumas et al., 2012). Piezoelectric vibration-based energy harvesting has an increasing importance nowadays especially due to the necessity of low power generation for charging mobile devices. Erturk & Inman (2011) presented a general overview of this subject, discussing the main concepts and applications of this idea. Recently, new aspects are being explored in order to enhance the energy harvesting system performance, allowing its use in new situations. In this regard, it is important to mention the influence of nonlinear effects (Silva et al., 2013) and random excitations (Litak et al., 2010; Martens et al., 2013; De Paula et al., 2015).

The inverse piezoelectric effect appears when the material is subjected to external electric fields causing changes in shape and size. This phenomenon is usually explored for actuation purposes (Flatau and Chong, 2002; Belouettar et al., 2008). Wang and Inman (2012, 2013) explored these two effects simultaneously for vibration control purposes. In essence, the harvested power is employed to control a mechanical system, reducing vibrations. Piezoelectric materials provided both the controller actuation and the harvested energy.

Nonlinear systems have an intrinsic richness and chaos is one of the possible responses of these systems. This kind of behavior has several typical characteristics that include sensitive dependence of initial conditions and the existence of an infinite number of unstable periodic orbits (UPOs). Chaos control exploits the richness embedded in chaotic behavior and may be understood as the use of small perturbations for the stabilization of an UPO. Since UPOs belong to the system dynamics, the stabilization of these orbits is associated with low power consumption. This idea can be employed to confer flexibility to the system and also to obtain systems with quick reaction to a specific stimulus (De Paula & Savi, 2011).

This paper deals with the use of chaos control using as the energy source the one harvested from available mechanical vibration. Piezoelectric materials provide both controller actuations and harvested energy. The combination of these two approaches may establish autonomous systems where available environmental mechanical energy can be employed for control purposes. The motivation to have a controller powered by a piezoelectric converter lies in the fact that chaos control has low power consumption. A piezomagnetoelastic bistable structure subjected to harmonic excitations is analyzed as a case study and two different goals can be defined as priority, allowing a change between them: vibration reduction and energy harvesting enhancement. Numerical simulations investigate different situations highlighting the ones where controller uses only the energy generated by the harvesting system.

This paper is organized as follows. The next section is dedicated to present chaos control methods. The third section shows the mathematical description of the system, while the fourth section presents numerical results. In the last section, conclusions are presented.

2 Chaos control methods

Chaos control may be understood as the use of small perturbations for the stabilization of Unstable Periodic Orbits (UPOs) embedded in a chaotic attractor. Since it is possible to stabilize system trajectories in different UPOs as needed, chaos control can lead to dynamical systems that may quickly react to new situations, changing conditions and their response. Therefore, this process is useful in several applications that require flexible system responses.

Typically, chaos control process occurs in two stages. The first one is the learning stage where the UPOs are identified and controller parameters are determined. The second one is the control stage, where perturbations are applied in order to stabilize the system response. Chaos control methods can be split into continuous and

discrete approaches. Continuous methods are based on the application of continuous-time perturbations to perform stabilization, while discrete methods seek to stabilize the system by means of non-continuous perturbations. De Paula & Savi (2011) presented a comparative analysis of the main chaos control methods showing that they have different characteristics associated with performance, robustness and capacity to stabilize UPOs. Therefore, a proper combination of methods can be employed to obtain a specific goal. Here, the Extended Time-Delayed Feedback method (ETDF) is employed as a continuous approach (Socolar et al., 1994) and the Semi-Continuous (SC) chaos control method proposed by Hübinger et al. (1994) is employed as a discrete approach. This combination is done in order to reach the stabilization of the desired UPOs. Concerning the learning stage, UPO identification is performed employing the close-return method (Auerbach, 1987).

2.1 Extended time-delayed feedback (ETDF) method

Pyragas (1992) presented a pioneer work proposing the application of continuous chaos control method, called Time Delayed Feedback method (TDF). Afterward, an extension of this method was proposed being called Extended Time-Delayed Feedback method (ETDF) (Socolar et al., 1994). For both cases, a dynamical system is governed by a set of nonlinear ordinary differential equations as follows:

$$\dot{x}(t) = Q(x,t) + B(t), \tag{1}$$

where t is time, $x(t) \in \Re^n$ is the state variable vector, $Q(x,t) \in \Re^n$ defines the system dynamics, while $B(t) \in \Re^n$ is the control action.

The ETDF control law considers information of time-delayed states of the system being represented by the following equations:

$$\begin{aligned} B(t) &= \mathbf{K}\left[(1-R)\,S_\tau - x\right] \\ S_\tau &= \sum\nolimits_{m=1}^{N_\tau} R^{m-1} x_{m\tau}, \end{aligned} \tag{2}$$

where $\mathbf{K} \in \Re^{nxn}$ is the feedback gain matrix, $0 \leq R < 1$ is a control gain, $S_\tau = S(t-\tau)$ and $x_{m\tau} = (t - m\tau)$ are related to delayed states of the system and τ is the time delay; N_τ establishes the number of delayed states considered in the analysis. In general, it is infinity but it can be properly defined depending on the dynamical system. The UPO stabilization can be achieved by an appropriate choice of $\mathbf{K}$ and R. Note that for any gain defined by $\mathbf{K}$ and R, perturbation of Eq.(2) vanishes when the system is on the UPO since $x(t - m\tau) = x(t)$ for all m if $\tau = T_i$, where T_i is the periodicity of the ith UPO. The ETDF is converted into the original TDF when $R = 0$.

The controlled dynamical system consists of a set of delayed differential equations (DDEs). The solution of this system is done by establishing an initial function $x_0 = x_0(t)$ over the interval $(-N_\tau\tau, 0)$. This function can be estimated by a Taylor series expansion as proposed by Cunningham (1954):

$$x_{m\tau} = x - m\tau\dot{x}. \tag{3}$$

Under this assumption, the following system is obtained:

$$\dot{x}(t) = Q(x,t) + K[(1-R)S_\tau - x] \tag{4}$$

$$\text{where} \begin{cases} S_\tau = \sum_{m=1}^{N_\tau} R^{m-1}\left[x - m\tau\dot{x}\right], & \text{for } (t - N_\tau\tau) < 0 \\ S_\tau = \sum_{m=1}^{N_\tau} R^{m-1} x_{m\tau}, & \text{for } (t - N_\tau\tau) \geq 0. \end{cases}$$

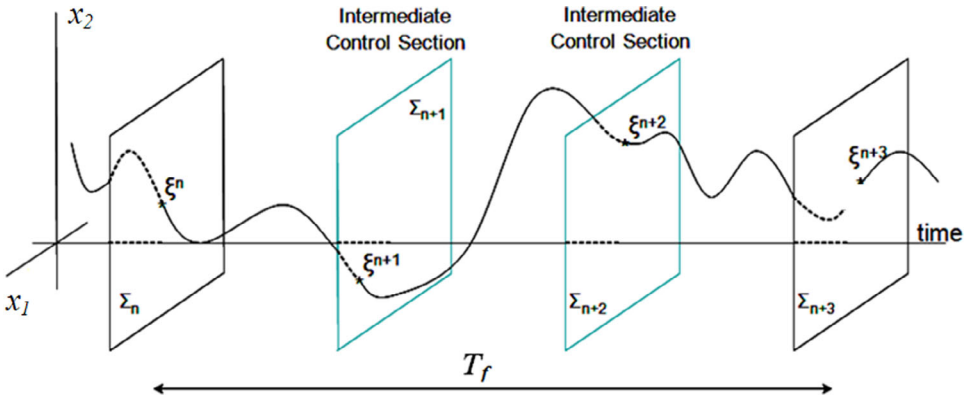

Fig. 1. Semi-continuous method (De Paula and Savi, 2011).

Note that DDEs contain derivatives that depend on the solution at delayed time instants. Therefore, besides the special treatment that must be given for $(t\text{-}N_\tau\tau) < 0$, it is necessary to deal with time-delayed states while integrating the system. A fourth-order Runge-Kutta method with linear interpolation on the delayed variables is employed for the numerical integration of the controlled dynamical system (Mensour & Longtin, 1997). It is important to note that the Taylor series expansion is used only at the beginning of the integration, while $(t\text{-}N_\tau\tau) < 0$, considering a proper number of terms. An alternative approach would adopt the start of the control action after all necessary delayed states are known, *i.e.*, when $t > N_\tau\tau$.

During the learning stage, it is important to define proper controller parameters, $\mathbf{K}$ and R, for each one of the desired UPOs. This is done by calculating the Lyapunov exponents of the correspondent orbit in such a way that exponents become all negatives, meaning that the UPO becomes stable.

2.2 Semi-continuous method (SC)

The semi-continuous method (SC) is a discrete chaos control method that lies between continuous and discrete time control. The discrete OGY method (Ott et al., 1990) considers one control station per forcing period, while the SC method introduces as many intermediate control stations as it is necessary to achieve stabilization of a desired UPO (Hübinger et al., 1994).

In order to use intermediate control stations per forcing period T, one introduces N equally spaced successive Poincaré sections $\Sigma_n, n = 0, ..., (N-1)$ as shown in Fig. 1. Let $\xi_C^n \in \Sigma_n$ be the intersections of the UPO with Σ_n and F be the mapping from one control station Σ_n to the next oneΣ_{n+1}.

The SC method is described by considering a discrete system of the form of a map $\xi^{n+1} = F(\xi^n, p^n)$, where $p \in \Re$ is an accessible parameter for control. This is equivalent to a parameter dependent map associated with a general surface, usually a Poincaré section. Let $\xi_C^{n+1} = F(\xi_C^n, p_0)$ denotes the unstable fixed point on this section corresponding to an unstable periodic orbit in the chaotic attractor that one wants to stabilize. During learning stage, the UPOs are identified, the control points ξ_c are determined and the sensitivity vectors, w^n, and the Jacobian matrices, J^n, are determined from time series analysis. The essential idea of the controller is to monitor the system dynamics until the neighborhood of this point is reached. Then, a proper small change of the parameter p causes the next state ξ^{n+1} to fall into the stable direction of the fixed point, v_s^{n+1}. The stabilization of the system is achieved

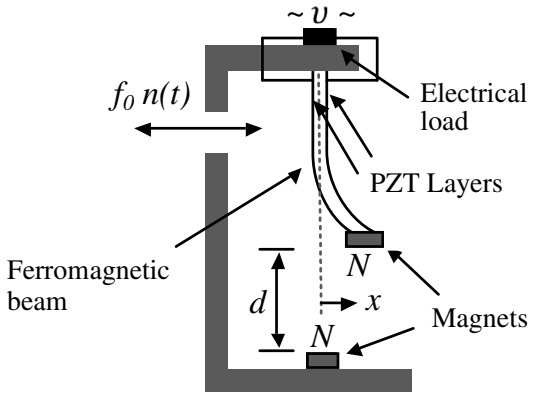

Fig. 2. Piezomagnetoelastic device (De Paula et al. 2015).

by considering proper values of scalars α and δp^n, estimated as follows (De Paula & Savi, 2011):

$$J^n \delta\xi^n + w^n \delta p^n = \alpha v_s^{n+1}, \tag{5}$$

where $\delta\xi^n = \xi^n - \xi_C^n$ and $\delta p^n = p^n - p_0$ correspond to the control actuation.

3 Piezomagnetoelastic structure

A piezomagnetoelastic structure is investigated as an energy harvesting system that one wants to control. This is a ferromagnetic cantilever beam with two permanent magnets, one located at the free end of the beam and the other at a vertical distance d from the beam free end. Two layers of piezoelectric materials are installed to the ferromagnetic beam, one in each side, operating with different goals as proposed by Wang and Inman (2012, 2013). Basically, one piezoceramic layer is used as energy harvester, $\mathrm{PZT_H}$, while the other is used as actuator, $\mathrm{PZT_C}$. The $\mathrm{PZT_H}$ layer is connected to the controller electrical circuit, while the $\mathrm{PZT_C}$ layer is connected to the harvester electrical circuit. Figure 2 presents a schematic picture of the system.

A simplified model of this energy harvesting system considers only one degree of freedom of the beam, denoted by x, corresponding to the tip displacement. System characteristics define its general behavior that can be related to either monostable or bistable system (De Paula et al., 2015). The bistable configuration is a typical Duffing-type system with double-well potential, being governed by the following equation (Erturk & Inman, 2008b, 2009; Erturk et al., 2008, 2009):

$$\ddot{x} + 2\xi\dot{x} - 0.5x + 0.5x^3 - \chi_1 v_1 - \chi_2 v_2 = f_0 \cos\Omega t \tag{6}$$

where x is the dimensionless displacement of the beam in the transverse direction, v_1 is the dimensionless voltage across the load circuit connected to the $\mathrm{PZT_H}$, v_2 is the dimensionless voltage across the load circuit connected to the $\mathrm{PZT_C}$, ξ is the mechanical viscous damping ratio, Ω is the dimensionless excitation frequency and χ_1 and χ_2 are the dimensionless piezoelectric coupling term in the mechanical equation for the layers of $\mathrm{PZT_H}$ and $\mathrm{PZT_C}$, respectively, being expressed as:

$$\chi_k = \frac{\theta_k}{M} \qquad (k = 1, 2) \tag{7}$$

where θ_k is the piezoelectric coupling device and M is the mass of the beam. In addition, electrical equation related to each piezoelectric layer is governed by (see for instance: Erturk et al., 2009):

$$c_k\dot{v}_k + i_k + \theta_k\dot{x} = 0 \qquad (k = 1, 2) \tag{8}$$

where c_k is the piezoelectric capacitance and i_k is the electric current of the external circuit. Dividing Eq. (8) by c_k and using $i_k = \left(\frac{v}{zc}\right)_k$, where z is the equivalent impedance considering the piezoelectric layer attached to the correspondent circuit, one obtains:

$$\dot{v}_1 + \mu_1 v_1 + \kappa_1\dot{x} = 0 \qquad (\mathrm{PZT_H}), \tag{9}$$

$$\dot{v}_2 + \mu_2 v_2 + \kappa_2\dot{x} = 0 \qquad (\mathrm{PZT_C}). \tag{10}$$

where $\mu_k = \left(\frac{1}{zc}\right)_k$ and $\kappa_k = \left(\frac{\theta}{c}\right)_k$.

The $\mathrm{PZT_C}$ layer provides control actuations and the control action, $B_{CONTROL}$, is applied to the correspondent state variable, v_2. Thus, the piezomagnetoelastic structure subjected to control is governed by the following equations:

$$\ddot{x} + 2\xi\dot{x} - 0.5x + 0.5x^3 - \chi_1 v_1 - \chi_2\left(v_2 + \frac{B_{CONTROL}}{\chi_2}\right) = f_0\cos\Omega t \tag{11}$$

$$\dot{v}_1 + \mu_1 v_1 + \kappa_1\dot{x} = 0, \tag{12}$$

$$\dot{v}_2 + \mu_2\left(v_2 + \frac{B_{CONTROL}}{\chi_2}\right) + \kappa_2\dot{x} = 0 \tag{13}$$

The control action of the ETDF is given by:

$$\begin{aligned} B_{CONTROL} &= K\left[(1-R)\,S_\tau - v_2\right] \\ S_\tau &= \sum\nolimits_{m=1}^{N_\tau} R^{m-1} v_{2_{m\tau}}. \end{aligned} \tag{14}$$

where K becomes a scalar. On the other hand, the semi-continuous control actions are defined from Eq. (5).

The performance of the proposed harvesting-control system is evaluated in terms of the electrical power consumed by the controller and the electrical power generated by the power harvester. The average electrical power is represented by:

$$P_{avg} = \frac{1}{T}\int_0^T P\,dt \tag{15}$$

where,

$$P = \frac{v^2}{z} \tag{16}$$

is the instantaneous electrical power. Note that two power values are evaluated: power harvested, P_H; controller power, P_C.

Table 1. System parameters.

Parameters	ξ	χ_1	μ_1	κ_1	χ_2	μ_2	κ_2
Values	0.01	0.05	0.05	0.50	0.05805	−2.07596	−0.00573

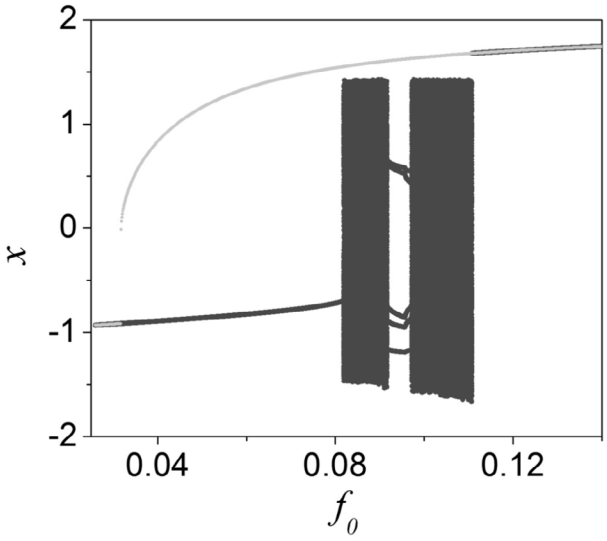

Fig. 3. Bifurcation diagram showing coexisting attractors.

4 Numerical simulations

Numerical simulations are performed showing the general behavior of the harvesting-control system. Parameters shown in Table 1 are employed for all simulations. Values of ξ, χ_1, λ_1 and κ_1 are obtained from Erturk et al. (2009), while values of χ_2, λ_2 and κ_2 are obtained from Wang and Inman (2012). Concerning the equivalent impedance, it is adopted 112 kΩ for the PZT_H circuit and 1.98 MΩ for the PZT_C circuit (Wang and Inman, 2013).

Initially, system behavior is evaluated considering an uncontrolled dynamics. Bifurcation diagram shows a stroboscopic view of the system response from a quasi-static variation of the forcing parameter f_0 when $\Omega = 0.8$ (Fig. 3). Note that for values of $f_0 < 0.03$ and $f_0 \geq 0.112$ the system presents a period-1 response, being related to a single point in the diagram. In the range of $0.03 \leq f_0 < 0.112$ system presents coexisting attractors, including periodic and non-periodic responses.

When $f_0 = 0.09$, a period-1 orbit coexists with a chaotic one, and this forcing parameter is analyzed in detail. A basin of attraction for this set of parameters is constructed and presented in Fig. 4. The two coexisting behaviors are represented with light gray points (period-1) and dark gray points (chaos). Figure 5 also shows these behaviors presenting both phase space and Poincaré section. Period-1 orbit is associated with initial conditions $(x(0), \dot{x}(0), v_1(0), v_2(0)) = (-1.63, 0.77, 0, 0)$, while chaotic response is related to $(x(0), \dot{x}(0), v_1(0), v_2(0)) =$(–1.63, –0.78,0,0).

Periodic and chaotic responses are confirmed by the Lyapunov exponents, λ, shown in Fig. 6. Period-1 behavior presents only negative values of Lyapunov exponents while chaotic behavior has one positive value.

Power harvested for each one of the previous attractors is now in focus considering both instantaneous electrical power harvested from PZT_H (in black) and average power (in gray) (Fig. 7). Note that average power harvested associated with periodic

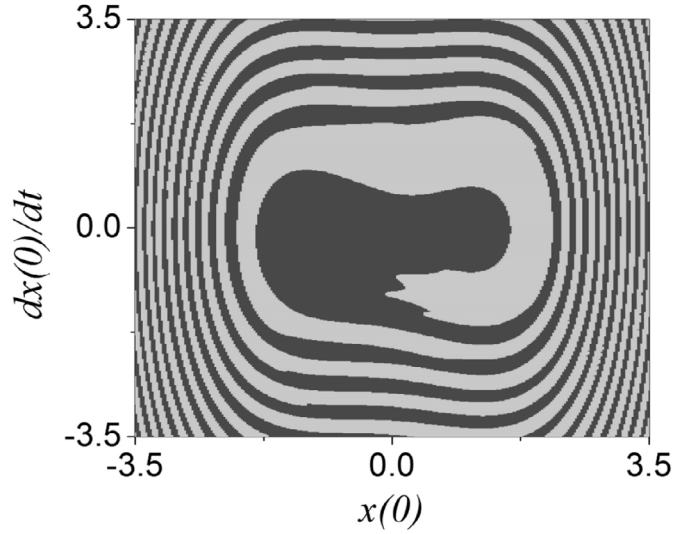

Fig. 4. Basin of attraction identifying two coexisting solutions: period one orbit (light gray points) and chaotic attractor (dark gray points).

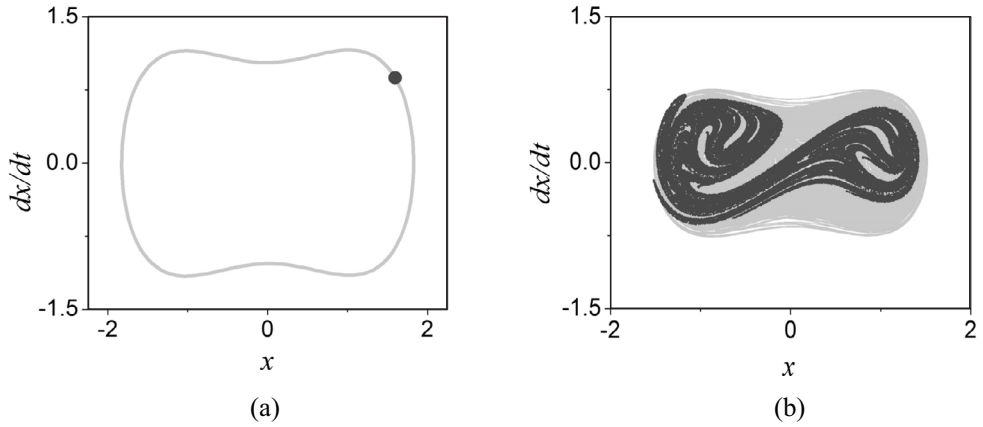

Fig. 5. Phase portrait and Poincaré section: (a) period-1; (b) chaos.

behavior is approximately 3.12×10^{-6}, while for the chaotic response presents an average power of 1.31×10^{-6}. Thus, comparing both responses for the uncontrolled system, the period-1 response has a better performance than the chaotic one for energy harvesting purpose, and this behavior is due to higher vibration amplitudes. Nevertheless, chaotic behavior can be exploited to confer flexibility to the system.

Control is now employed in order to exploit chaotic behavior to obtain a flexible system that can be used to perform either energy harvesting or vibration reduction. An interesting characteristic of this system is that the power harvested is employed to supply the controller needs. The same chaotic behavior presented in the previous results is employed in the forthcoming analysis. Initially, a learning stage is of concern, identifying UPOs and defining controller parameters. The close-return method (Auerbach, 1987) is employed for this aim, and three unstable orbits are identified: period-1; period-2; a different period-2. These three

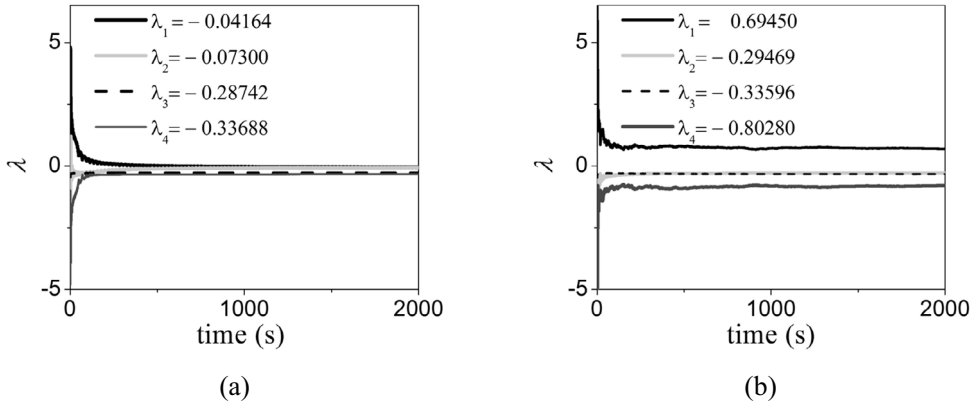

Fig. 6. Lyapunov exponents of the two coexisting attractors: (a) period-1; (b) chaos.

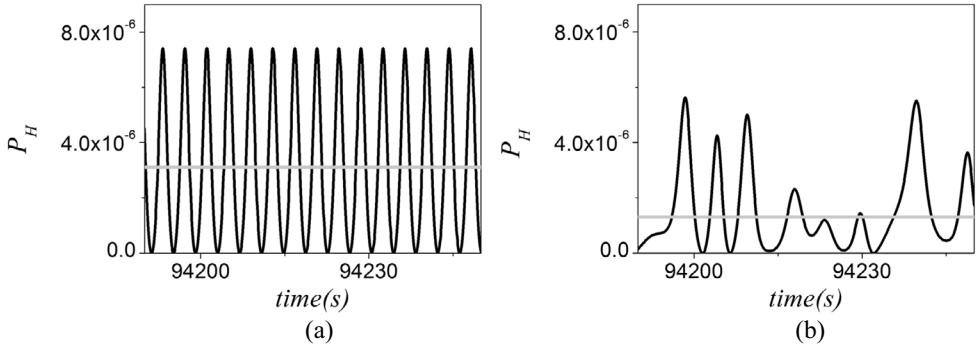

Fig. 7. Instantaneous and average harvested electric power from: (a) period 1 orbit; (b) chaotic response.

orbits are presented together with the determination of Lyapunov exponents employed for controller parameters determination of the ETDF (Figs. 8–10). Period-1 orbit is presented in Fig. 8; period-2 orbit is shown in Fig. 9 while the other period-2 orbit is presented in Fig. 10. It should be pointed out that, based on vibration amplitude arguments, it is possible to choose one of these orbits based on the desired application. For instance, the first two orbits have small amplitudes and therefore, are interesting for situations where low vibration amplitudes are needed. The last one is related to large amplitudes and therefore can be used for energy harvesting purposes. Hence, the chaotic response can confer this flexibility if it is possible to choose, using some controller, the most interesting orbit.

Chaos control is now focused on establishing a system response related to different UPOs. Initially, period-1 UPO, shown in Fig. 8, is of concern. Figure 11 shows the stabilization using ETDF method with $R = 0.1$ and $K = 0.6$ presenting: steady-state phase space; control signal; instantaneous (black) and average (gray) harvested power; and instantaneous (black) and average (gray) power used by the control actuations. The average electrical power consumed by the controller for the stabilization of this UPO is approximately 1.34×10^{-6}, while the average harvested electrical power is 3.49×10^{-7}. Hence, the piezoelectric converter provides 26% of the power consumed by the controller.

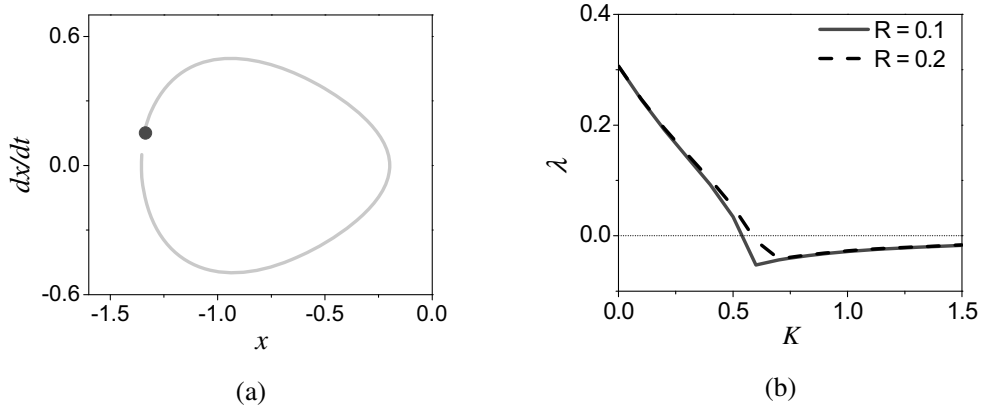

Fig. 8. (a) Period-1 UPO selected for vibration reduction purpose; (b) maximum Lyapunov exponents for different values of R and K.

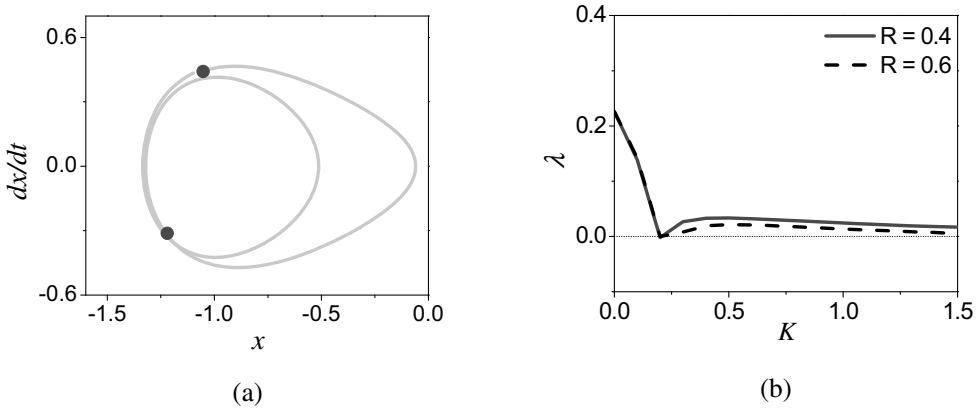

Fig. 9. (a) Period-2 UPO selected for vibration reduction purpose; (b) maximum Lyapunov exponents for different values of R and K.

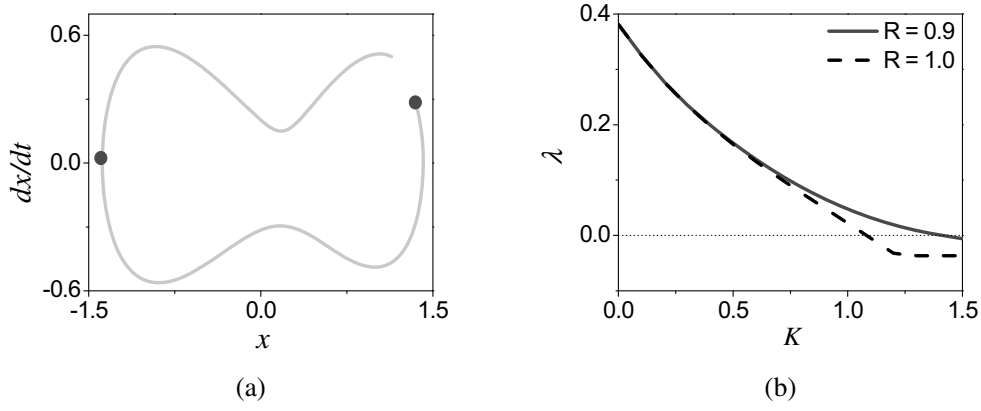

Fig. 10. (a) Period-1 UPO selected for energy harvesting purpose; (b) maximum Lyapunov exponents for different values of R and K.

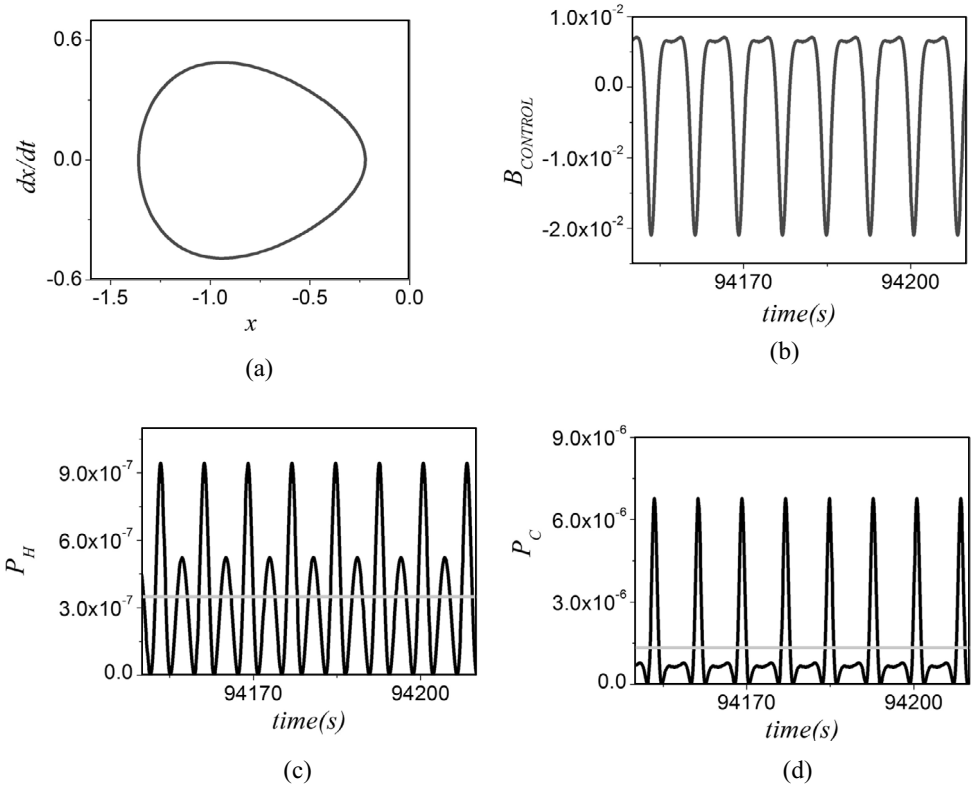

Fig. 11. ETDF method stabilization of period-1 UPO orbit with $R = 0.1$ and $K = 0.6$: (a) steady state phase space; (b) control signal; (c) power harvested; and (d) power consumed by the controller.

Figure 12 shows the stabilization of the period-2 UPO. Once again, ETDF method is employed with $R = 0.6$ and $K = 0.2$ and steady-state phase space, control signal, instantaneous (black) and average (gray) harvested power and instantaneous (black) and average (gray) power used by the control actuations are presented. The normalized average electrical power consumed by the controller to stabilize the UPO is approximately 2.79×10^{-6}, while the average harvested electrical power is 3.71×10^{-7}. Hence, the piezoelectric converter provides 13% of the power consumed by the controller.

The second period-2 UPO (Fig. 10), attractive for energy harvesting purposes due to its large amplitude, is not able to be stabilized using the ETDF method. Although there are negative values of Lyapunov exponents, the ETDF is not effective for this goal. De Paula & Savi (2001) discussed some aspects related to the efficacy of chaos control methods to stabilize UPOs pointing some alternatives to achieve this goal. A possible alternative is the use of the semi-continuous method that is applied in the sequence.

The learning stage of the SC method identifies the UPO using the same approach of the ETDF. Afterward, sensitivity vectors and Jacobian matrices are calculated. Five control stations per forcing period are considered. The control stage considers a wait time until the system trajectory falls in the neighborhood of the desired UPO, when the controller is turned on. Figure 13 presents the UPO stabilization, showing steady-state phase space, control signal, instantaneous (black) and average (gray)

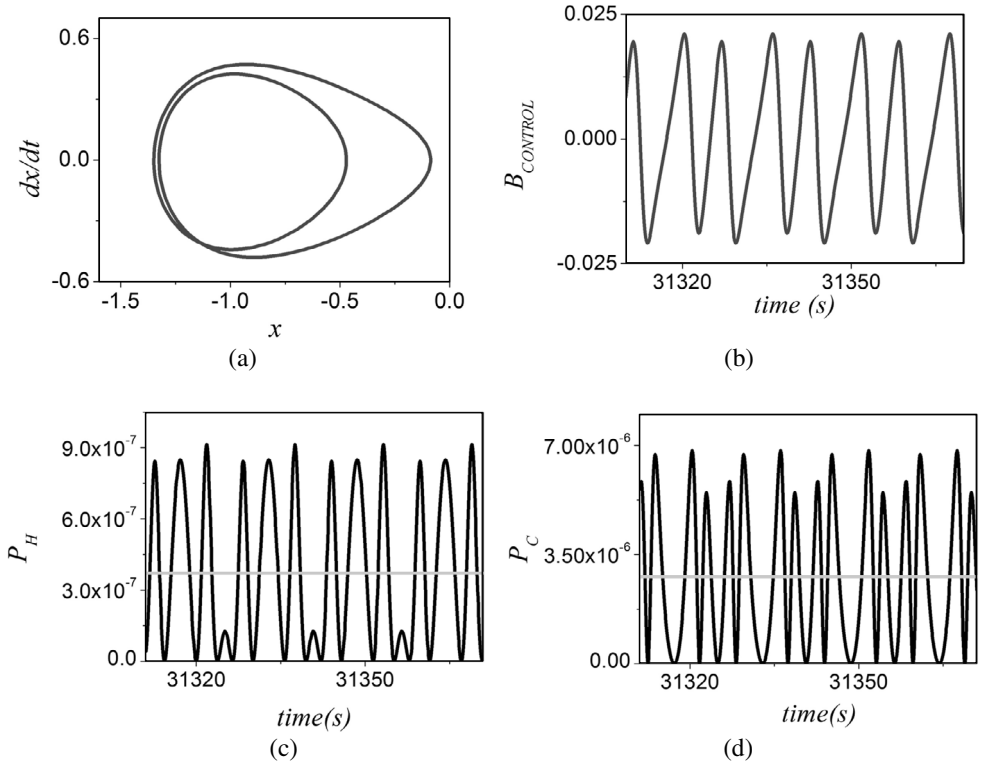

Fig. 12. ETDF method stabilization of period-2 UPO for vibration reduction purpose with $R = 0.6$ and $K = 0.2$: (a) steady-state phase space; (b) control signal; (c) power harvested; and (d) power consumed by the controller.

harvested power and instantaneous (black) and average (gray) power used for control actuations. The non-dimensional average electrical power consumed by the controller when stabilizing the UPO is approximately 2.77×10^{-7}, while the average harvested electrical power is 1.46×10^{-6}. Hence, the power generated by the piezoelectric converter is greater than the power consumed by the controller. Subtracting the average harvested power by the power consumed by the controller, one obtains 1.183×10^{-6} of net harvested power, which correspond around 90% of the harvested power obtained by the chaotic response without control (Fig. 7b).

The semi-continuous method is now employed to stabilize the other identified period-1 UPO (Fig. 8 and Fig. 11). The idea is to observe the difference between SC and ETDF methods trying to establish a proper combination of procedures in order to obtain better controller performance. Figure 14 presents results of the stabilization showing the steady-state phase space, control signal, instantaneous (black) and average (gray) harvested power and instantaneous (black) and average (gray) power used for control actuations. The non-dimensional average electrical power consumed by the controller when stabilizing the UPO is approximately 1.83×10^{-7}, while the average harvested electrical power is 3.62×10^{-7}. The net harvested power is now 1.79×10^{-7} corresponding around 14% of the harvested power obtained by the chaotic response without control. It is important to highlight that the main goal, when vibration reduction is of concern, is the use of the harvested power to supply the controller and not to use the net harvested power. Here, different from the ETDF use, the

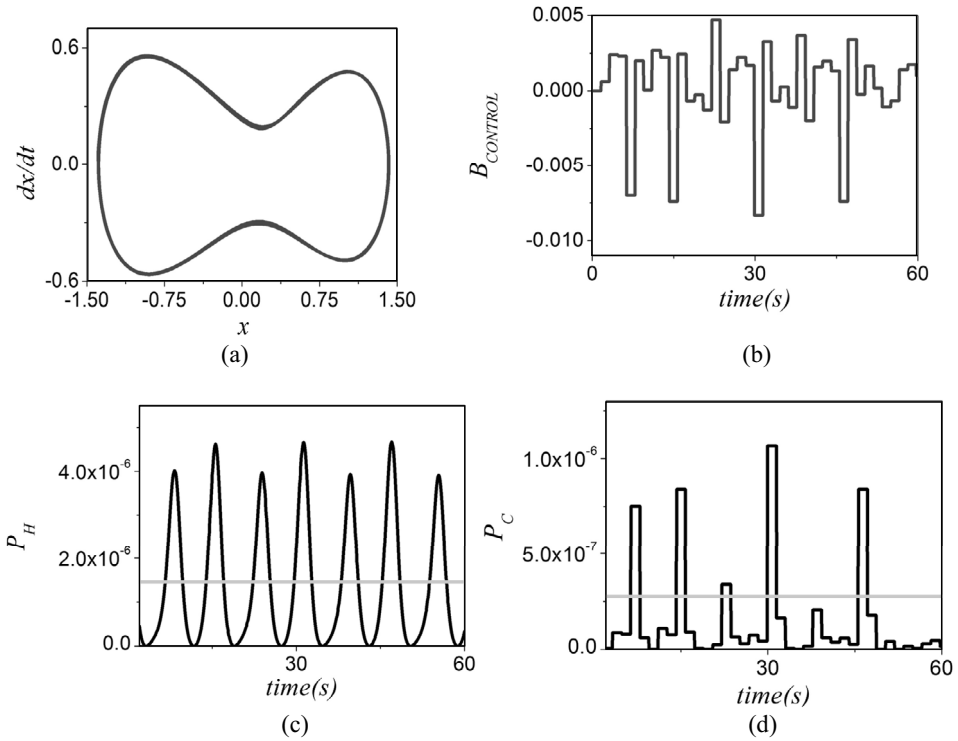

Fig. 13. SC method stabilization of period-2 UPO for energy harvesting purpose: (a) steady-state phase space; (b) control signal; (c) power harvested; and (d) power consumed by the controller.

harvested power is enough to fully supply the controller and there is still a net harvested power. Therefore, the performance of the SC is more interesting than the ETDF since the proposed harvester-controller system presents energy autonomy.

Results showed that the combination of chaos control and energy harvesting can be an useful approach. Due to the characteristics of chaos control methods it is interesting to establish a combination of procedures in order to define a proper performance. ETDF is usually more robust but it is not able to stabilize all UPOs. On the other hand, SC has a better efficacy, spending less energy. Therefore, it is possible to think in terms of a controller exploring the proper characteristic of each method. As the studied system is high dimensional, the SC method can have difficulties in stabilizing the desired UPO. Once again, the combination can be interesting.

5 Conclusions

This work deals with the application of chaos control in energy harvesting systems. The main idea is to combine chaos control and energy harvesting exploiting the system flexibility in order to change from various desired UPOs embedded in a chaotic attractor. In addition, controller power can be fully or partially provided by the energy harvesting system. In this regard, two priority goals can be identified: vibration reduction and energy harvesting enhancement. Two control methods are employed allowing a combination for UPO stabilization: extended time-delay feedback (ETDF) and semi-continuous (SC). UPOS are identified during the learning stage and three

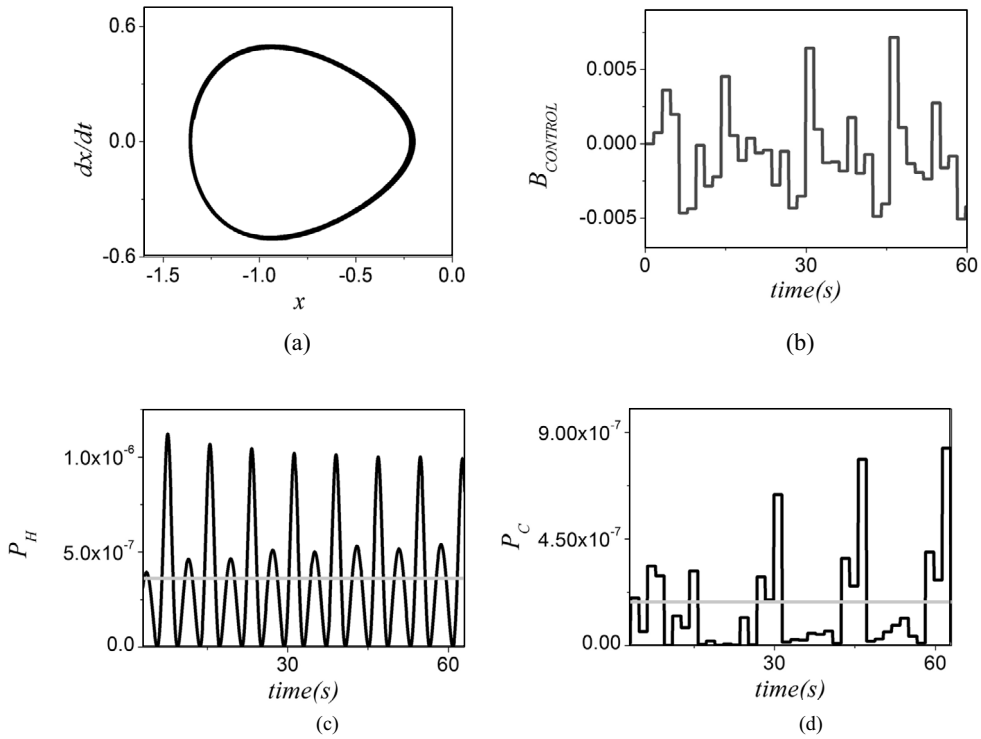

Fig. 14. SC method stabilization of period-1 UPO for energy harvesting purpose: (a) steady-state phase space; (b) control signal; (c) power harvested; and (d) power consumed by the controller.

situations are investigated. The UPO stabilization can define several interesting situations. Some of them are more convenient in terms of vibration reduction and the controller power supply is partially or fully provided by the power harvester. Some other situations, related to higher vibration amplitudes, can provide the whole power needed for the controller and the net harvested power can be storage or applied to other purposes. Therefore, the combination of chaos control and energy harvesting can be useful for different situations. The use of chaos control makes possible the change among several different situations, according to the needs of a given application.

The authors would like to thank the Brazilian Research Agencies CNPq, CAPES and FAPERJ and through the INCT-EIE (National Institute of Science and Technology−Smart Structures in Engineering) the CNPq and FAPEMIG for their support. The authors would like also to acknowledge the support of ANP, FINEP and MCT through PRH-PB/MCT, and also the support of Petrobrás.

References

1. D. Auerbach, P. Cvitanovic, J.P. Eckmann, G. Gunaratne, I. Procaccia, Phys. Rev. Lett. **58**, 2387 (1987)
2. S. Belouettar, L. Azrar, E.M. Daya, V. Laptev, M. Potier-Ferry, Computers and Structures **86**, 386 (2008)
3. W.J. Cunningham, Mathematics **40**, 708 (1954)

4. A.S. De Paula, A.S. Savi, International J. Non-linear Mechanics **46**, 1076 (2011)
5. A.S. De Paula, D.J. Inman, M.A. Savi, Mech. Syst. Signal Proc. **54**, 405 (2015)
6. A. Erturk, D.J. Inman, Smart Mater. Struct. **17**, 065016 (2008a)
7. A. Erturk, D.J. Inman, ASME J. Vibr. Acoust. **130**, 041002 (2008b)
8. A. Erturk, D.J. Inman, Smart Mater. Struct. **18**, 025009 (2009)
9. A. Erturk, D.J. Inman, *Piezoelectric energy harvesting* (Wiley, 2011)
10. A. Erturk, O. Bilgen, D.J. Inman, Appl. Phys. Lett. **93**, 224102 (2008)
11. A. Erturk, J. Hoffmann, D.J. Inman, Appl. Phys. Lett. **94**, 2541102 (2009)
12. A.B. Flatau, K.P. Chong, Eng. Struct. **24**, 261 (2002)
13. K. Gkoumas, O.D. Gaudenzi, F. Petrini, Procedia – Social Behav. Sci. **48**, 1097 (2012)
14. B. Hübinger, R. Doerner, W. Martienssen, M. Herdering, R. Pitka, U. Dressler, Phys. Rev. E **50**, 932 (1994)
15. D.J. Leo, Hobokeb (New Jersey: John Wiley & Sons, 2007)
16. G. Litak, M.I. Friswell, S. Adhikari, Appl. Phys. Lett. **96**, 214103 (2010)
17. W. Martens, U. von Wagner, G. Litak, Eur. Phys. J. Special Topics **222**, 1665 (2013)
18. B. Mensour, A. Longtin, Physica D **113**, 1 (1997)
19. E. Ott, C. Grebogi, J.A. Yorke, Phys. Rev. Lett. **64**, 1196 (1990)
20. K. Pyragas, Phys. Lett. A **170**, 421 (1992)
21. L.L. Silva, M.A. Savi, P.C.C. Monteiro Jr., T.A. Netto, J. Intell. Mater. Syst. Struct. **24**, 1278 (2013)
22. J.E.S. Socolar, D.W. Sukow, D.J. Gauthier, Phys. Rev. E **50**, 3245 (1994)
23. L. Tang, Y. Yang, C.K. Soh, J. Intelli. Materi. Syst. Struct. **21**, 1867 (2010)
24. Y. Wang, D.J. Inman, IEEE/ASME Trans. Mechatr. **18**, 1289 (2013)
25. Y. Wang, D.J. Inman, J. Composite Mater. **47**, 125 (2012)